

**Study of nuclei identification**  
**with**  
**AMS02 silicon ladders**

**Chih-hsun LIN**  
**National Central University, Taiwan**

# 1. Introduction

The performance of AMS02 silicon ladders for detecting nuclei has been studied by beam tests at CERN and GSI in 2003. There were six AMS02 silicon ladders exposed to heavy ion beams. Each ladder consists several double sides, K and S, silicon strip detectors. The readout pitch is  $208\ \mu\text{m}$  for the K-side and  $110\ \mu\text{m}$  for the S-side. The sketch of the experimental setup is shown in Figure 1. The distance between each ladder was  $50\pm 1\ \text{mm}$ . All six ladders were placed in perpendicular to beams. In addition, the AMS02 RICH prototype was also tested together with AMS02 silicon ladders at CERN. The charge measured by the RICH prototype can be used to verify results from AMS02 silicon ladders.

The beam type of CERN was a fragmentation beam produced by a primary Indium beam with  $158\ \text{GeV}/u$  beam energy. The ions were selected according to the ratio of atomic mass ( $A$ ) and atomic charge ( $Z$ ). Two values were used in the test,  $A/Z = 2$  and  $A/Z = 2.25$ . Tests at GSI were made with Boron and Carbon beams at  $0.8\ \text{GeV}/u$ . The beam profiles of CERN and GSI, shown in Figure 2, were less than two readout chips (128 readout channels). Therefore, only one readout chip in each side of each ladder was considered in the analysis.

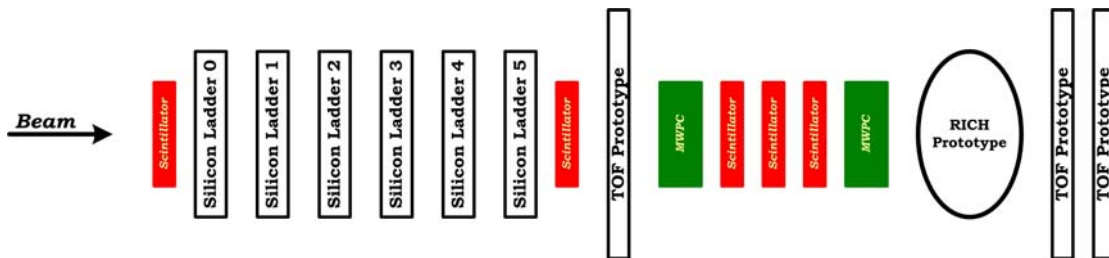


Figure 1: Sketch of the experimental setup for the beam tests. There were only AMS02 silicon ladders at the GSI tests.

## 2. Analysis

### 2.1. Cluster reconstruction

The ionization energy generated by a charged particle in a silicon ladder is collected by a cluster of adjacent strips. The energy measured by each readout channel is subtracted for the common mode shift and pedestal value. The common mode shift represents the mean of the uniform shift over channels of a readout chip. The random-triggered events with the common mode shift subtracted are used to

determine the pedestal value of each channel; the mean is the pedestal and the width is the noise,  $\sigma_n$ . The pedestal value is around 500 ADC counts. The distributions of  $\sigma_n$  of six ladders are plotted in Figure 3. The average value of  $\sigma_n$  is about 2.5 ADC counts for the S-side and 3.0 ADC counts for the K-side, which is in agreement with one measured in the laboratory.

A cluster is defined by following selections:

- A cluster must contain the channel with maximum energy of one side of a ladder. Its energy must be greater than  $3\sigma_n$ .
- The neighboring channels with energy greater than  $1.5\sigma_n$  are included in a cluster. For the K-side, the energy ordering requirement is also applied. For the S-side, one channel below the  $1.5\sigma_n$  threshold is allowed in the both left and right sides of a cluster in order to overcome a problem of triple or double peaks structure in a cluster reported by *reference 1*.
- The integral energy of a cluster is required to be larger than 15 ADC counts for the S-side and 20 ADC counts for the K-side.

Figure 4 and Figure 5 show the distributions of integral cluster energy for the K- and S-sides of a ladder. The double peak structure is observed in several energy regions associated to different ions for the K- and S-sides. The overlap between adjacent ions is also significant. The cluster energy collected at the K- and S-sides is quite different for ions with  $Z$  greater than two because of different gains.

## 2.2. Corrections to cluster energy

The cluster energy is identified to be dependent on the impact position of a charged particle. Figure 6 and Figure 7 show the average of the cluster energy as a function of the particle impact position for different ions<sup>1</sup>. The particle impact position is represented by the centre-of-gravity of a cluster,  $COG$ , defined as:

$$COG = \frac{\sum iQ_i}{\sum Q_i} - 0.05 \dots\dots\dots(1)$$

where  $i$  is the channel number of a strip in the cluster and  $Q_i$  is its energy. The constant shift 0.05 at  $COG$  is to make the average of the cluster energy symmetric respected to  $COG$  at 0.5. The  $COG$  dependence of the cluster energy is different between the K- and S-sides. It also varies with different ions (cluster energies), except

---

<sup>1</sup> The ions are identified by using results with corrected cluster energy shown at end of this section.

for low  $Z$  ions at the K-side and high  $Z$  ions at the S-side where the  $COG$  dependences of the cluster energy are similar among different ions. One reason for this variation with ions is the effect of saturation, which affects mainly for clusters at the K-side. The energy of the single channel can not be greater than about 3400 ADC counts<sup>2</sup>. Figure 8 shows the distribution of the energy of the peak channel of a cluster at the K-side for different ions as an example. This limit is due to the gain setting in front-end electronics, which is set to prevent the overflow in the analog-digital converter.

To improve the ion identification, the cluster energy has to be corrected according to the  $COG$  and cluster energy. The correct factors with the  $COG$  and cluster energy dependence are estimated as follows:

A. For the K-side:

- A1. Estimate the correction factor with the  $COG$  dependence only by the Carbon data of the GSI test first. The  $COG$  region,  $0.45 \leq COG \leq 0.55$ , is used as the reference for the calculation of correct factors.
- A2. Apply these  $COG$  dependent only correction factors to the CERN data. Since they are independent to the cluster energy, clusters affected by the effect of saturation have to be rejected by a cut (3000 ADC counts) on the peak channel energy of a cluster.
- A3. Transfer the corrected cluster energy of each ladder from the ADC unit to the charge ( $Z$ ) unit to equalize the gain difference between different readout chips. Then the results from different ladders are combined to have the average charge measurement,  $\bar{Z}$ , as:

$$\bar{Z} = \frac{1}{n-2} \left[ \sum_{i=1}^n Z_i - Z^{Max} - Z^{Min} \right]$$

$$\sigma^2(\bar{Z}) = \frac{1}{n-3} \left[ \sum_{i=1}^n (Z_i - \bar{Z})^2 - (Z^{Max} - \bar{Z})^2 - (Z^{Min} - \bar{Z})^2 \right] \dots (2)$$

where  $n$  is the number of ladders. It is required to be larger than four. The error of combined  $Z$  value,  $\sigma^2(\bar{Z})$ , is also calculated event by event.

---

<sup>2</sup> In other word, the limit at the energy of a channel without the pedestal and common mode shift subtraction is close to 4000 ADC counts.

- A4. The combined  $Z$  value is used to identify ions for each ladder in order to re-estimate the correction factor with the  $COG$  and cluster energy dependence. The dependence of  $COG$  is estimated bin by bin (20 bins). The cluster energy dependence is estimated by the polynomial fit for each  $COG$  bin.
- A5. Apply the new correction factor to the data and combine the results from different ladders again as mentioned in Step A3. If there are more ions identified, repeat Step A3 to Step A5.
- B. For the S-side:
  - B1. Use the combined  $Z$  value measured at the K-side to identify ions.
  - B2. Estimate the correction factor with the  $COG$  and cluster energy dependence.
  - B3. Apply the correction factor to the data and combine the results from different ladders as mentioned in Step A3.

The correction factors are calculated for each ladder. Figure 9 and Figure 10 show the energy dependence of the correction factor in different  $COG$  bins. The dependence is similar among different  $COG$  bins, but the variation becomes smaller when the  $COG$  bin is close to 0.5.

### 2.3. Charge ( $Z$ ) measurements

Figure 11 shows the corrected cluster energy distribution of a ladder. The contributions from individual ions are also shown. The ion identification at the K-side is better than the S-side. With a single ladder, the ions can be identified up to Silicon ( $Z=14$ ). Above  $Z=14$ , the overlap among ions in the cluster energy distribution is significant because of the effect of resolution. For the S-side, the overlap in the corrected cluster energy distribution is also serious from Boron ( $Z=5$ ) to Neon ( $Z=10$ ). It is due to the gain transition as shown in Figure 12 of the square root of corrected cluster energy versus  $Z$ . The measured cluster energy at the S- and K-sides follows basically the  $Z^2$  relation. For the S-side, there are two linear regions with a factor of two difference in gain. The exact reason for the gain variation at the S-side is unknown. For the K-side, the slope of the  $Z^2$  relation is changed around  $Z=14$  because of the saturation effect.

The measured  $Z$  values from different ladders are combined for both the S- and K-sides by using the method mentioned above. To reject events with large angle

scattering and improve the result, the following selections are applied:

- Number of ladders used in the charge measurement must be larger than four for both the S- and K-sides.
- The  $\chi^2$  of the linear tracking fit is required to be less than 6000 for both the S- and K-sides.
- The difference between combined  $Z$  values from the S- and K-sides is required to be less than one. This selection is illustrated in Figure 13, which shows the correlation of combined  $Z$  between two sides of silicon ladders.

The combined  $Z$  measurements are shown in Figure 14. The ions can be identified up to Iron ( $Z=26$ ) at the K-side and Argon ( $Z=18$ ) at the S-side with combined results from six ladders. The spectrums of the combined  $Z$  measurement are fitted by the Gaussian function for each ion. In order to improve the fit, the contributions from beam fragment events and the non-Gaussian tail of each ion are parameterized by the polynomial. The results of the fit are also shown in Figure 14. For ions with the Gaussian sigma greater than 0.2, their spectrum is well reproduced by the Gaussian fit and the contribution of non-Gaussian tails from neighboring ions is negligible. The Gaussian sigma of each ion is shown in Figure 15 and is compared to the average error of combined  $Z$  values calculated by Equation 2. Figure 16 shows the correlations of measured  $Z$  values from the RICH prototype [2], the K- and S-side of silicon ladders. The good correlation is observed up to Iron ( $Z=26$ ). The resolution of charge measurement of the K-side is also compatible with the RICH prototype. The average size of a cluster at the K- and S-sides is shown in Figure 17 as a function of measured  $Z$ . It increases with  $Z$  increasing and is consistent among different ladders.

### **3. Conclusions**

The performance of AMS02 silicon ladders for detecting nuclei has been verified by beam tests at CERN and GSI in 2003. With combined results of six silicon ladders, the ions can be identified up to Iron ( $Z=26$ ). The results agree the measurements of RICH prototype.

### **Acknowledgements**

We wish to thank Geneva University group for their support and useful discussions to this analysis.

## Reference

- [1] P. Azzarello, Ph. D thesis in preparation.
- [2] RICH presentations in TEM, April 2004.

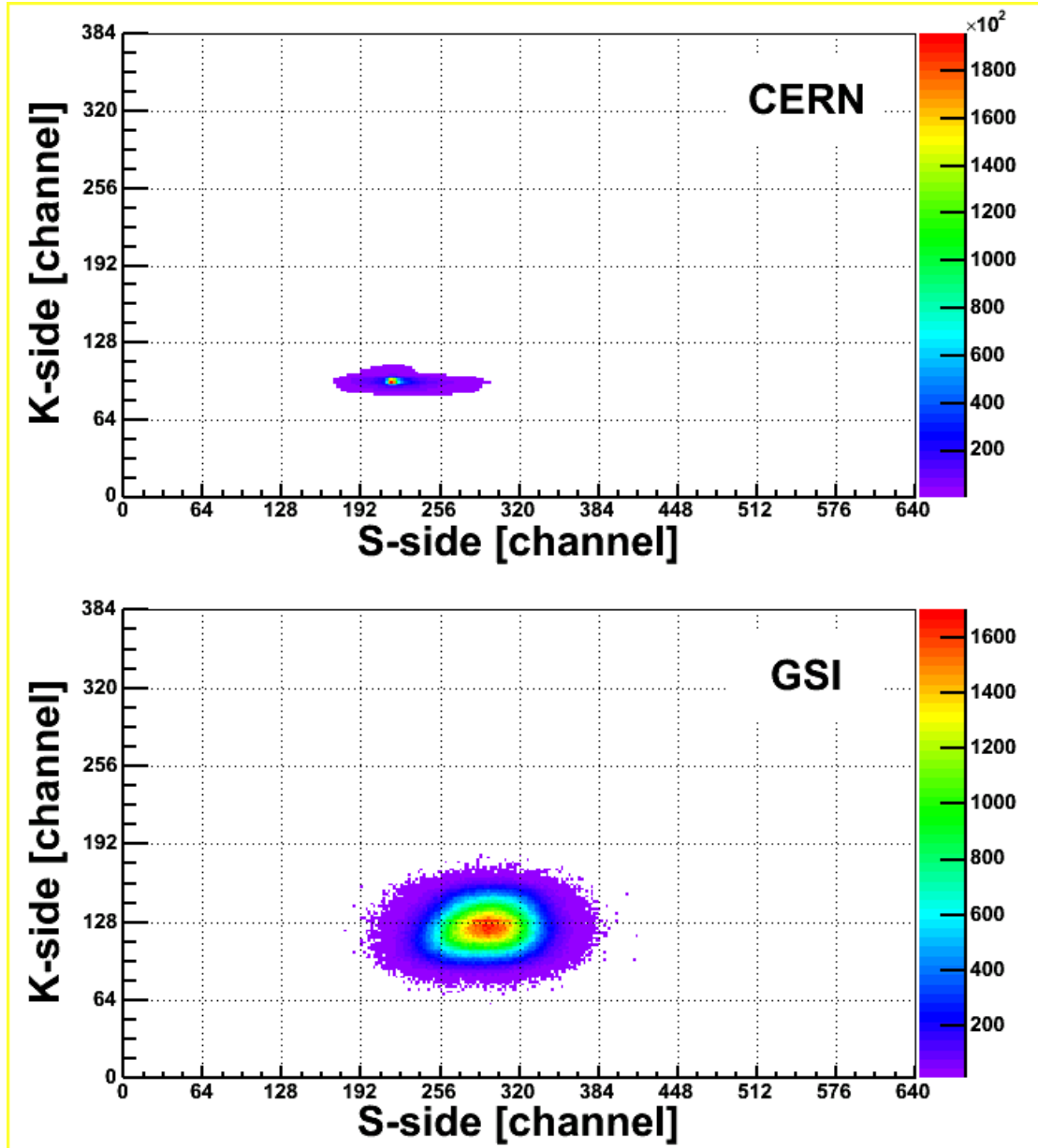


Figure 2: Profile of CERN and GSI beams. The width of beams is less than two readout chips at the both K- and S-sides.

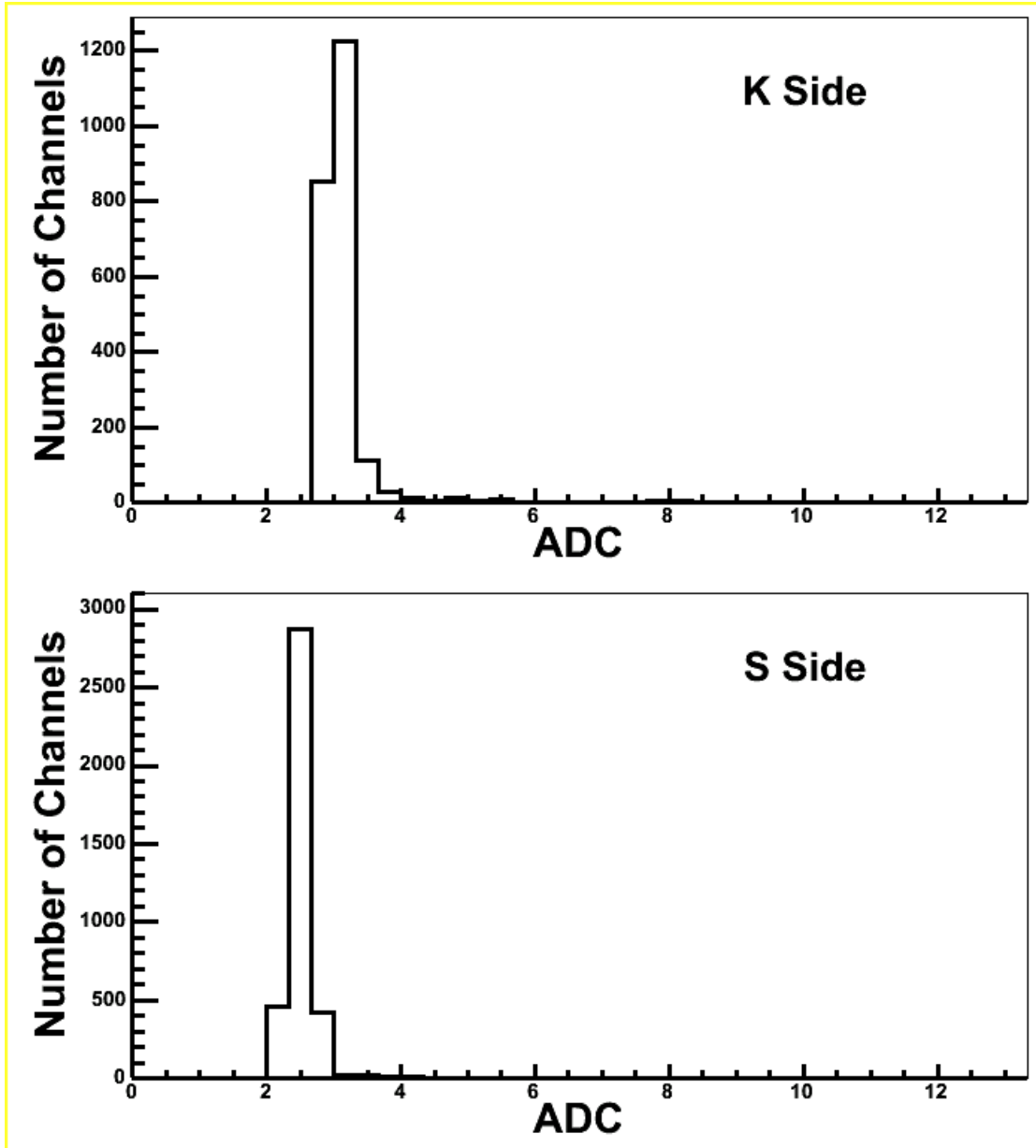


Figure 3: Noise distributions of the K- and S-side of silicon ladders.

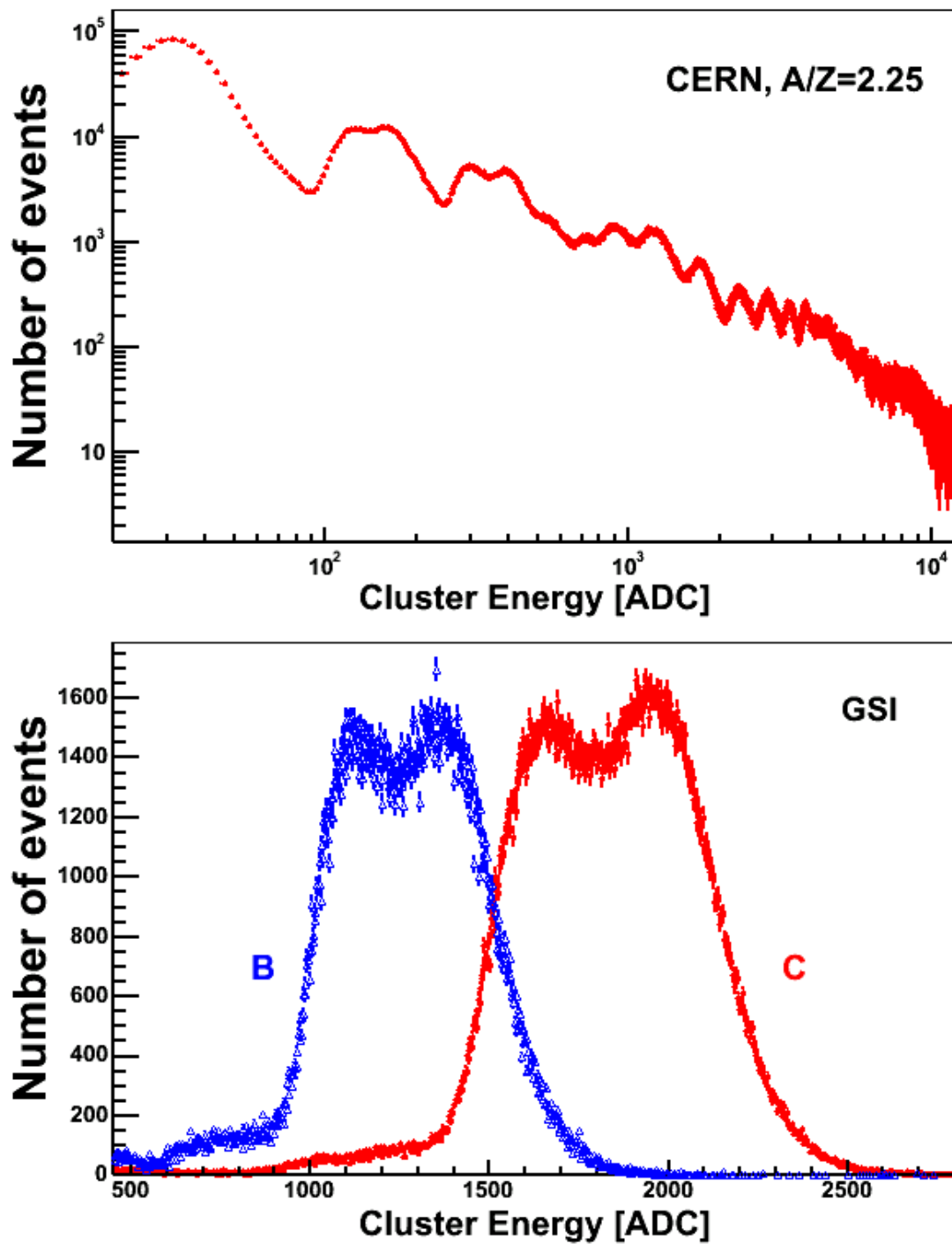


Figure 4: Cluster energy distributions of the K-side of a single ladder.

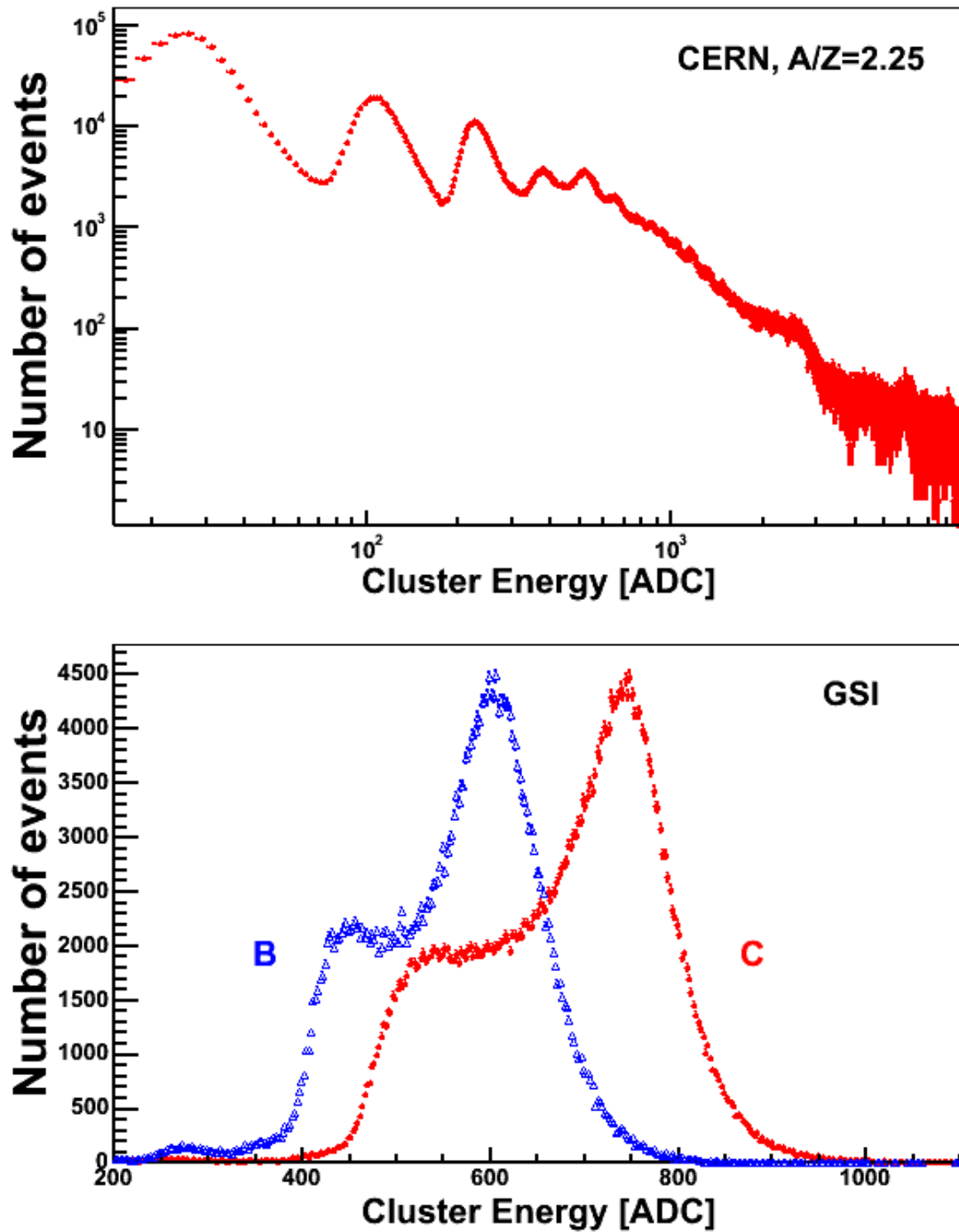


Figure 5: Cluster energy distributions of the S-side of a single ladder.

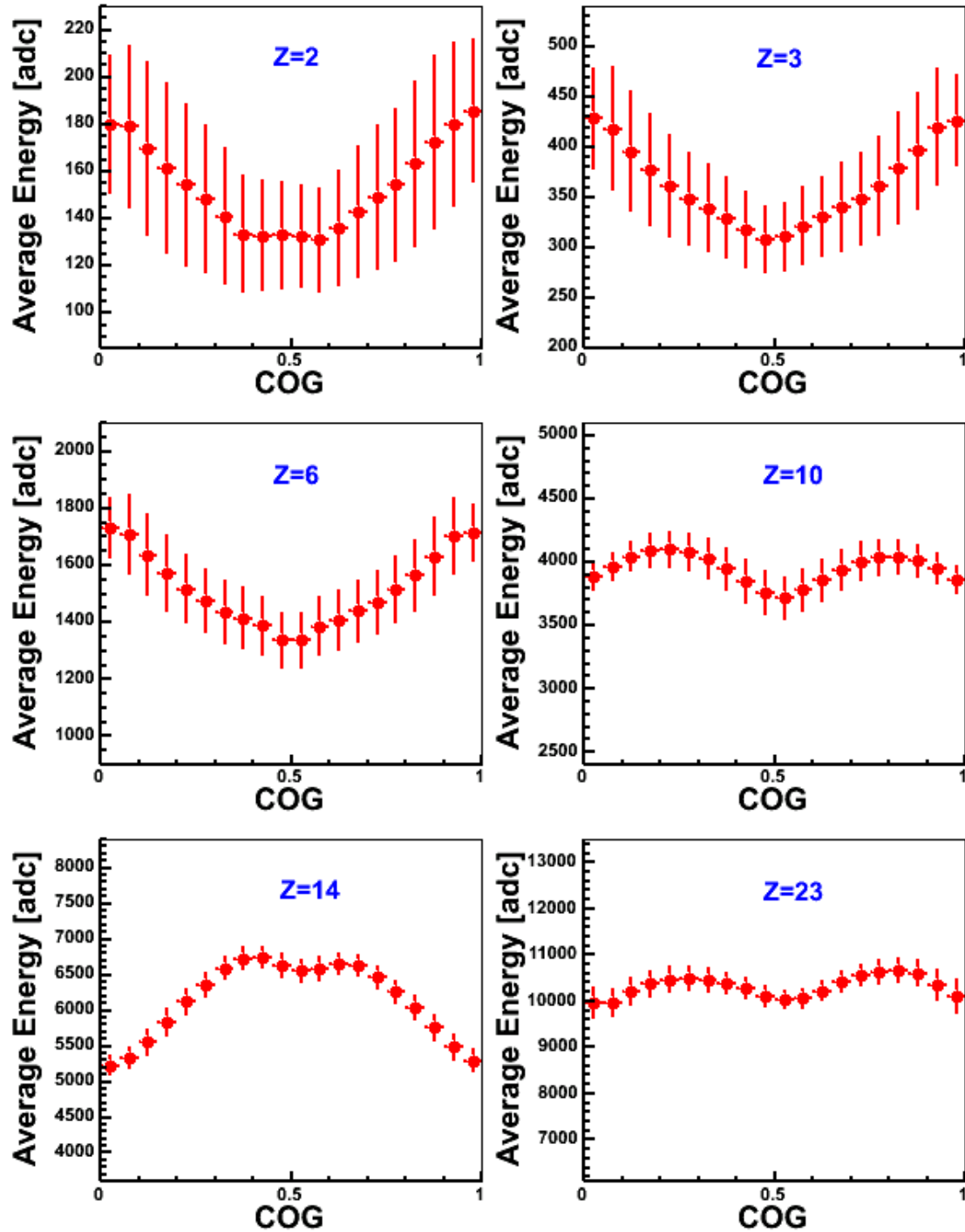


Figure 6: Average cluster energies as a function of COG at the K-side of a silicon ladder for different types of ions.

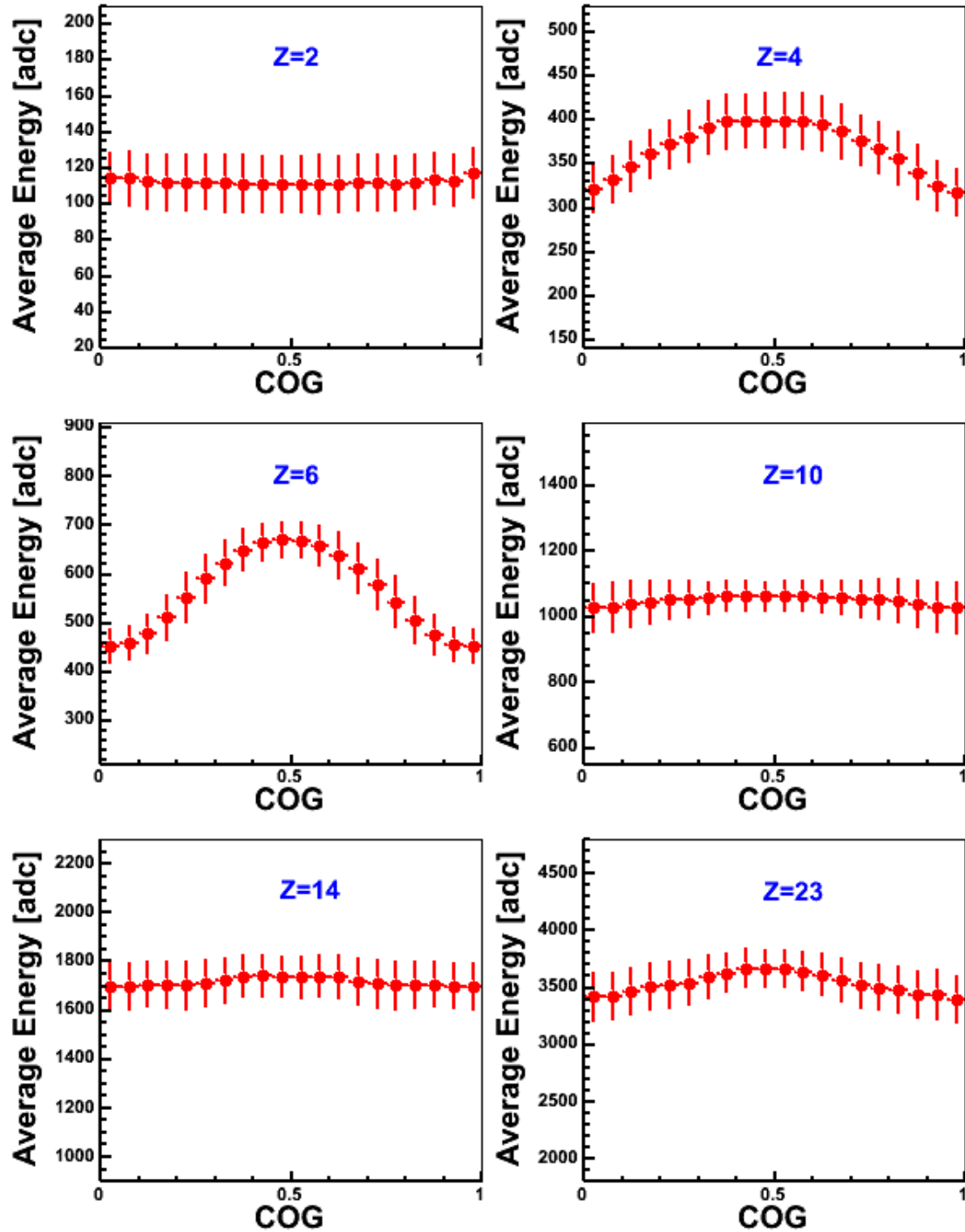


Figure 7: Average cluster energies as a function of COG at the S-side of a silicon ladder for different types of ions.

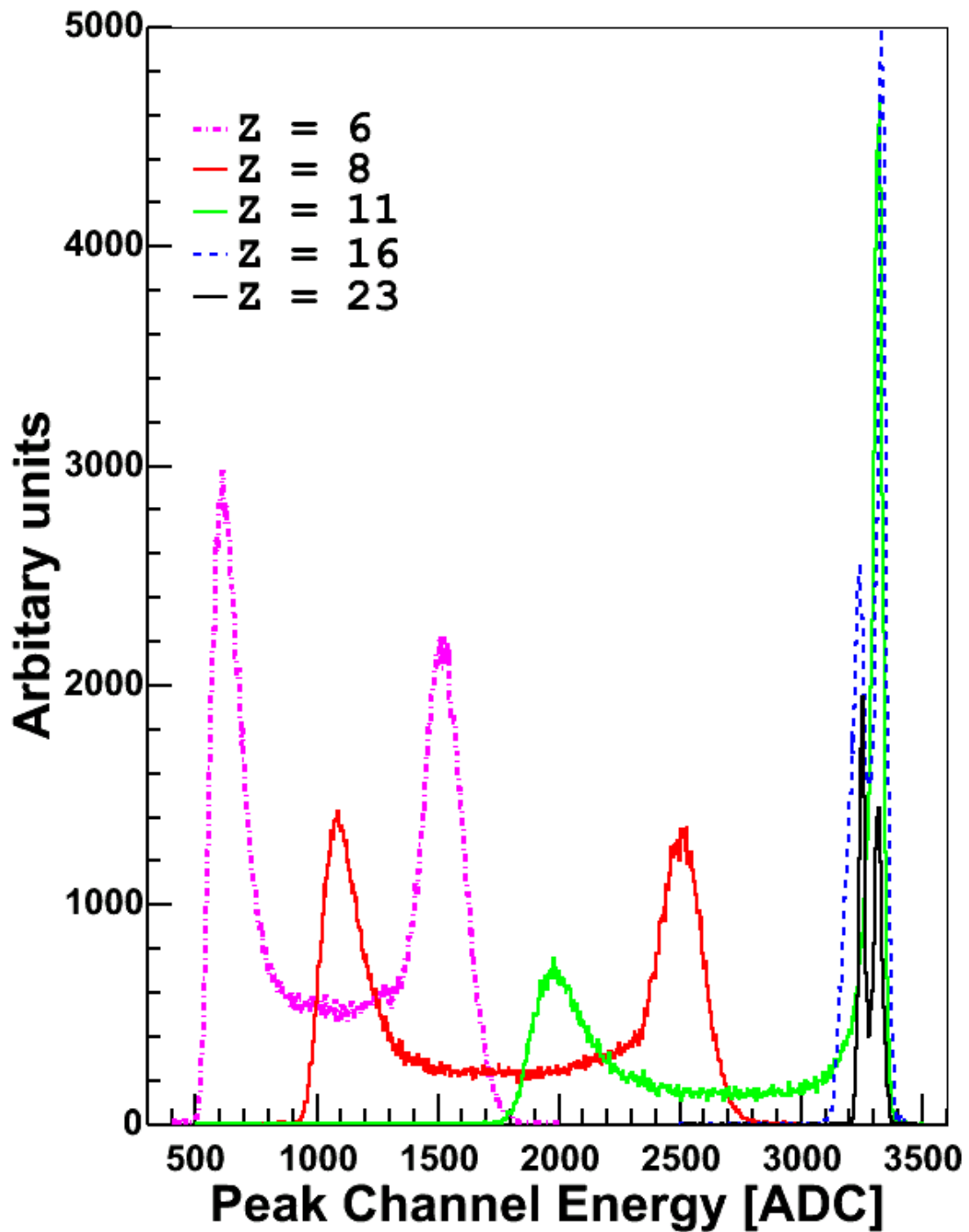


Figure 8: Distributions of the peak channel energy of a cluster at the K-side for different types of ions. The limit is about 3400 ADC counts.

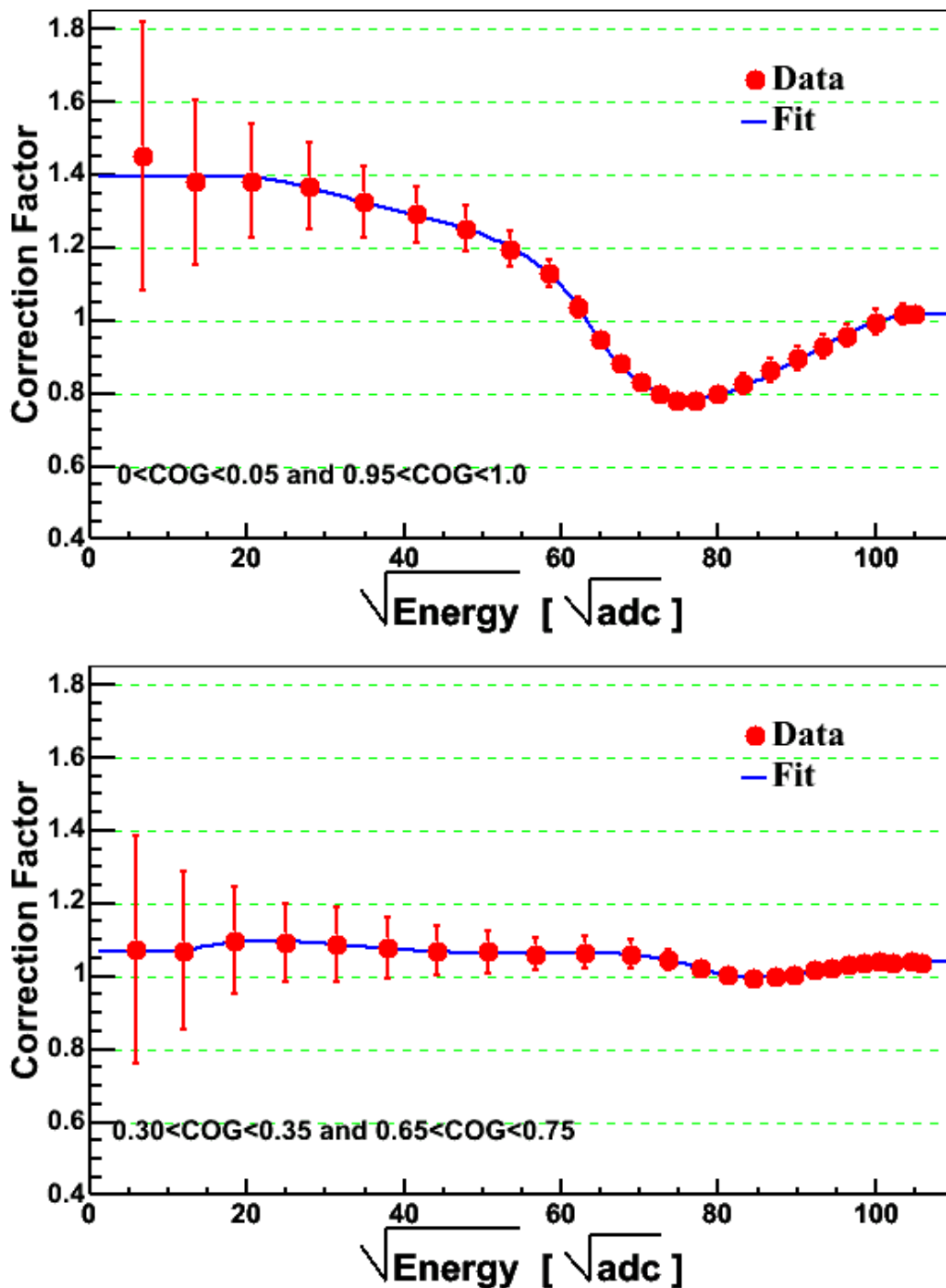


Figure 9: Cluster energy dependence of the correction factor of the K-side at two different COG regions.

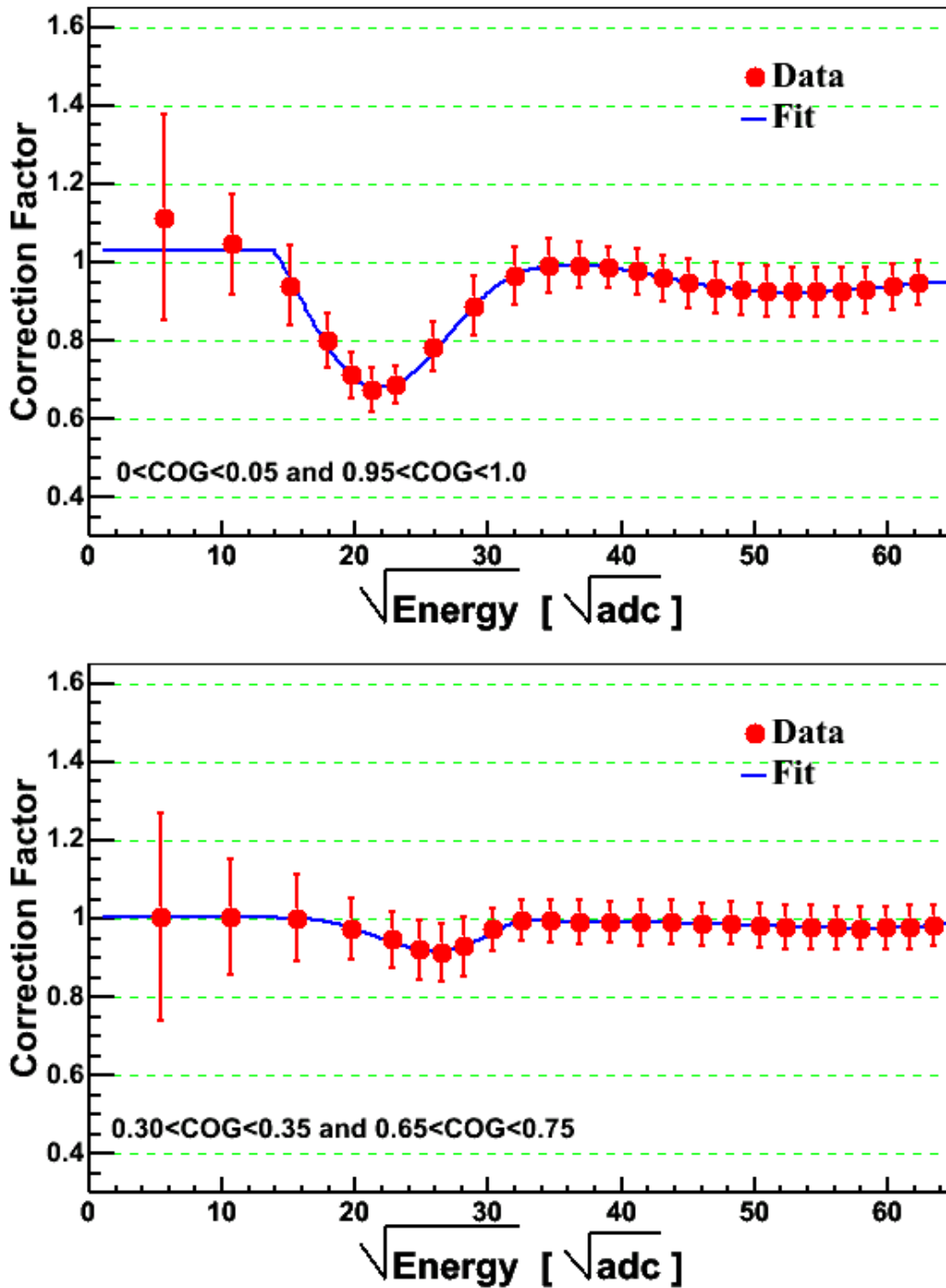


Figure 10: Cluster energy dependence of the correction factor of the S-side at two different COG regions.

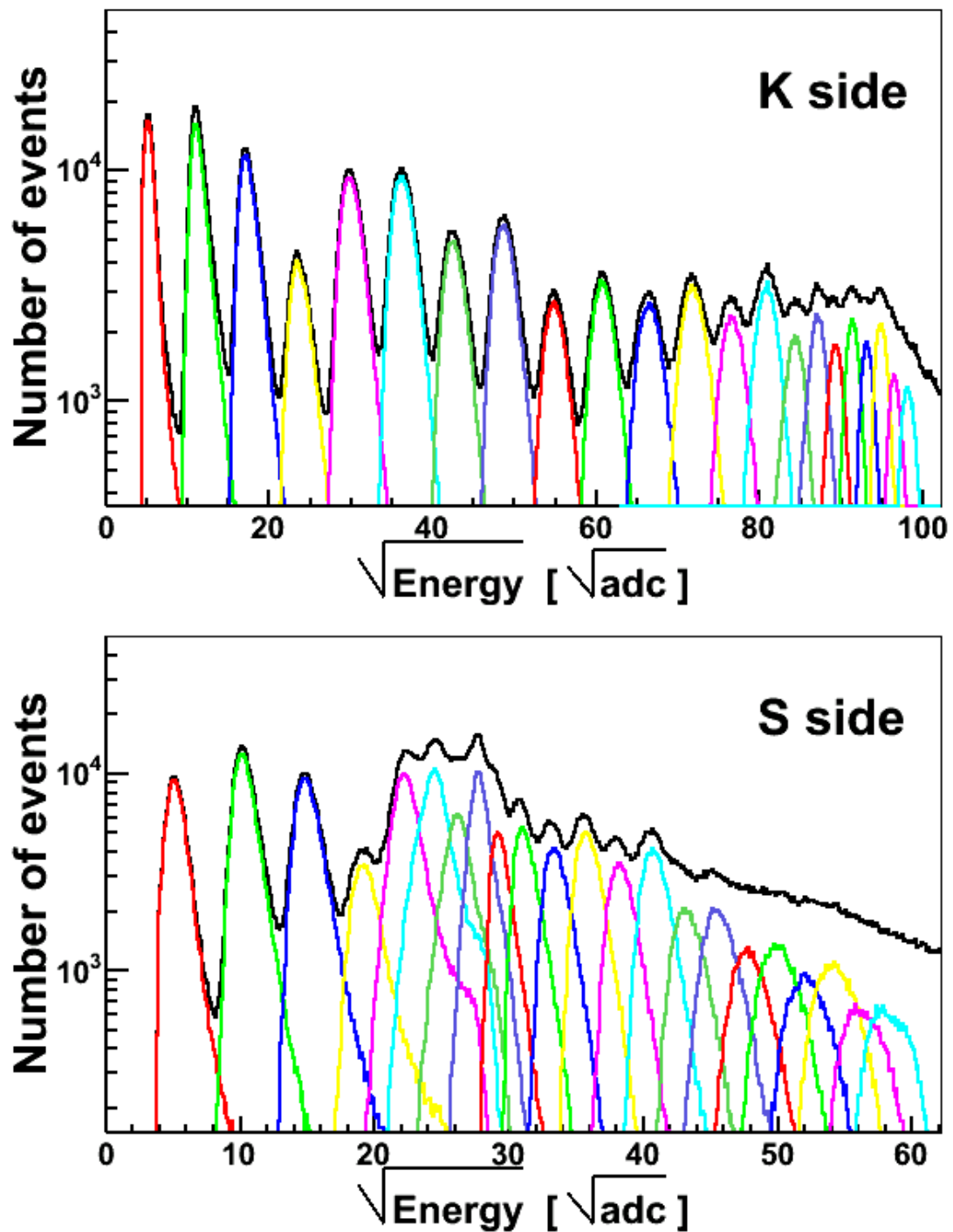


Figure 11: Distributions of corrected cluster energies of the K- and S-sides of a single ladder. The contributions from individual ions are also shown.

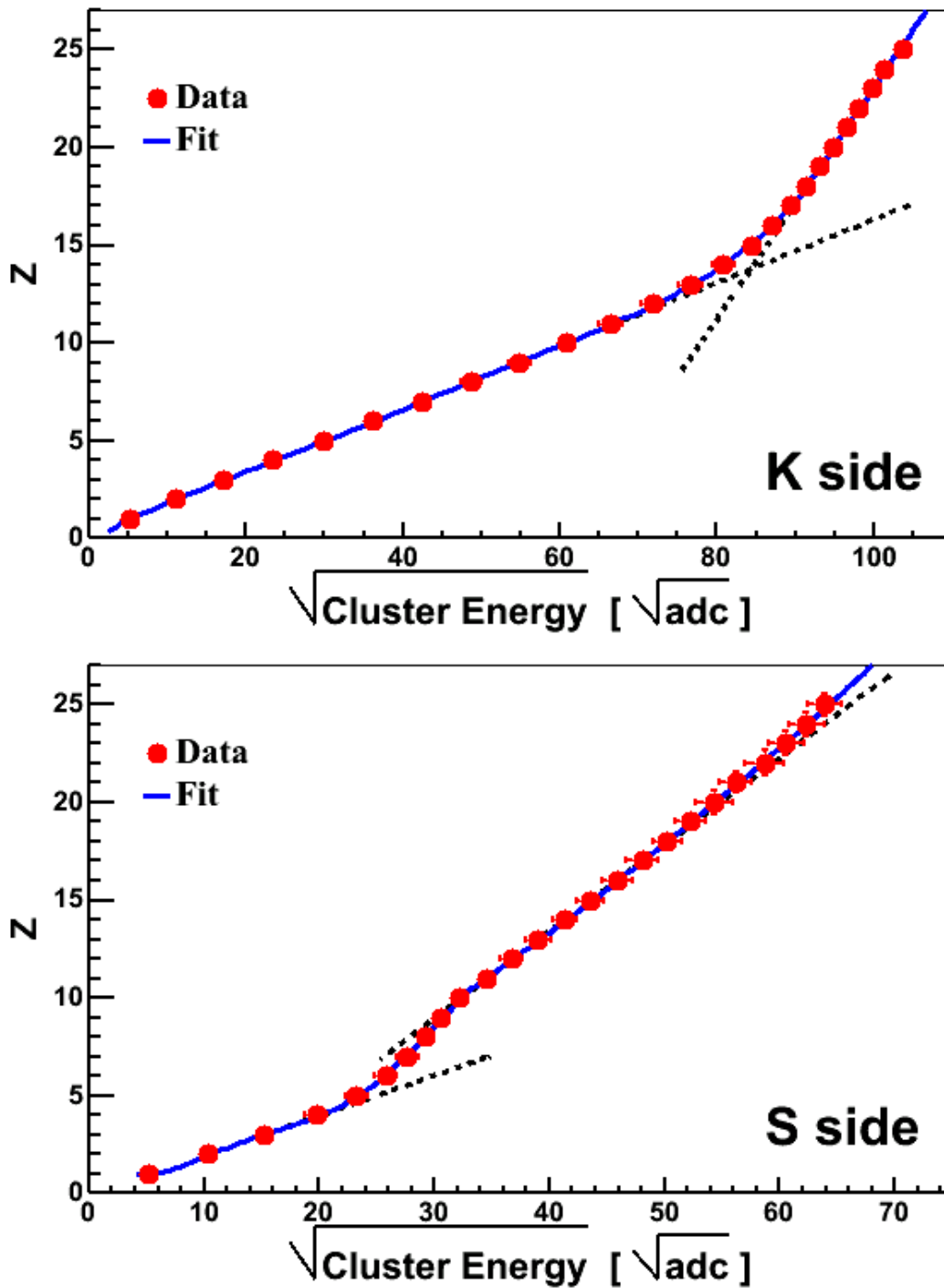


Figure 12: Correlation between the charge and the corrected cluster energy at the K- and S-sides.

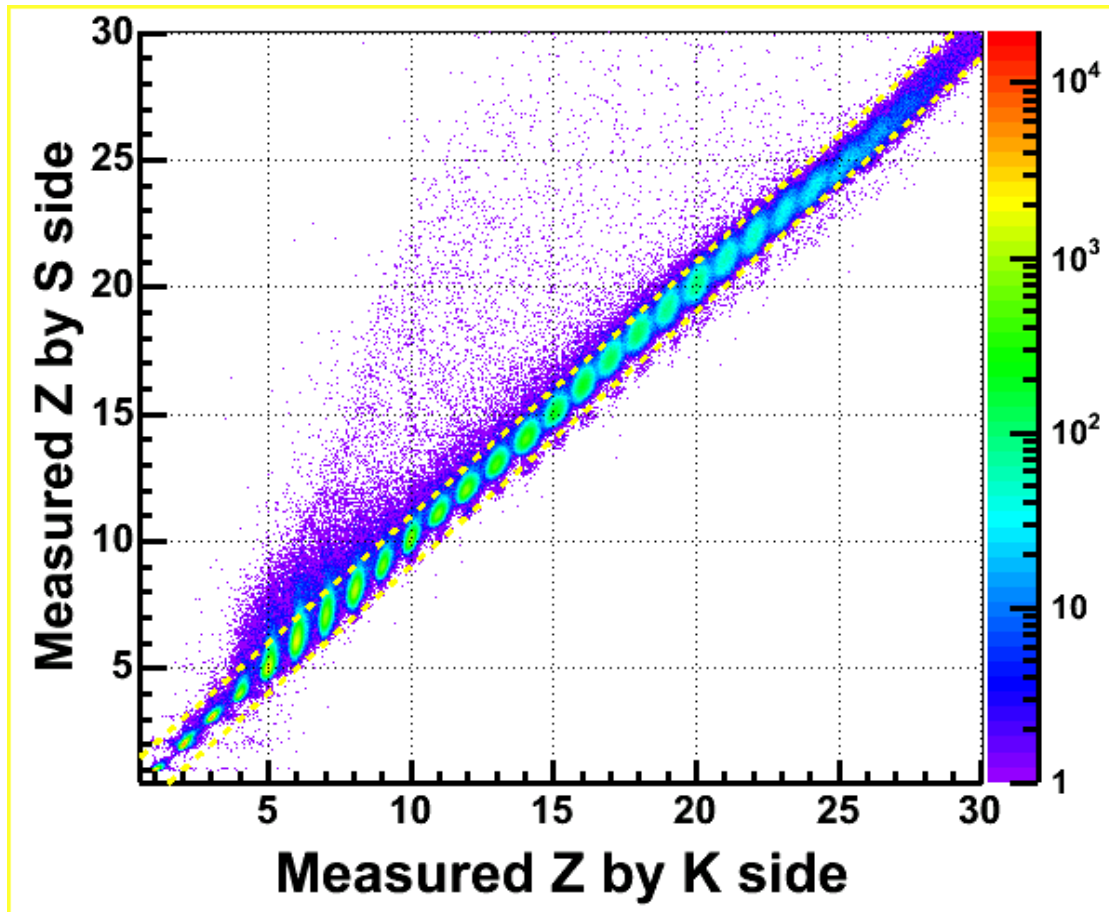


Figure 13: Correlation between charges measured by the K- and S-sides. The dash line represents the selection described in the text.

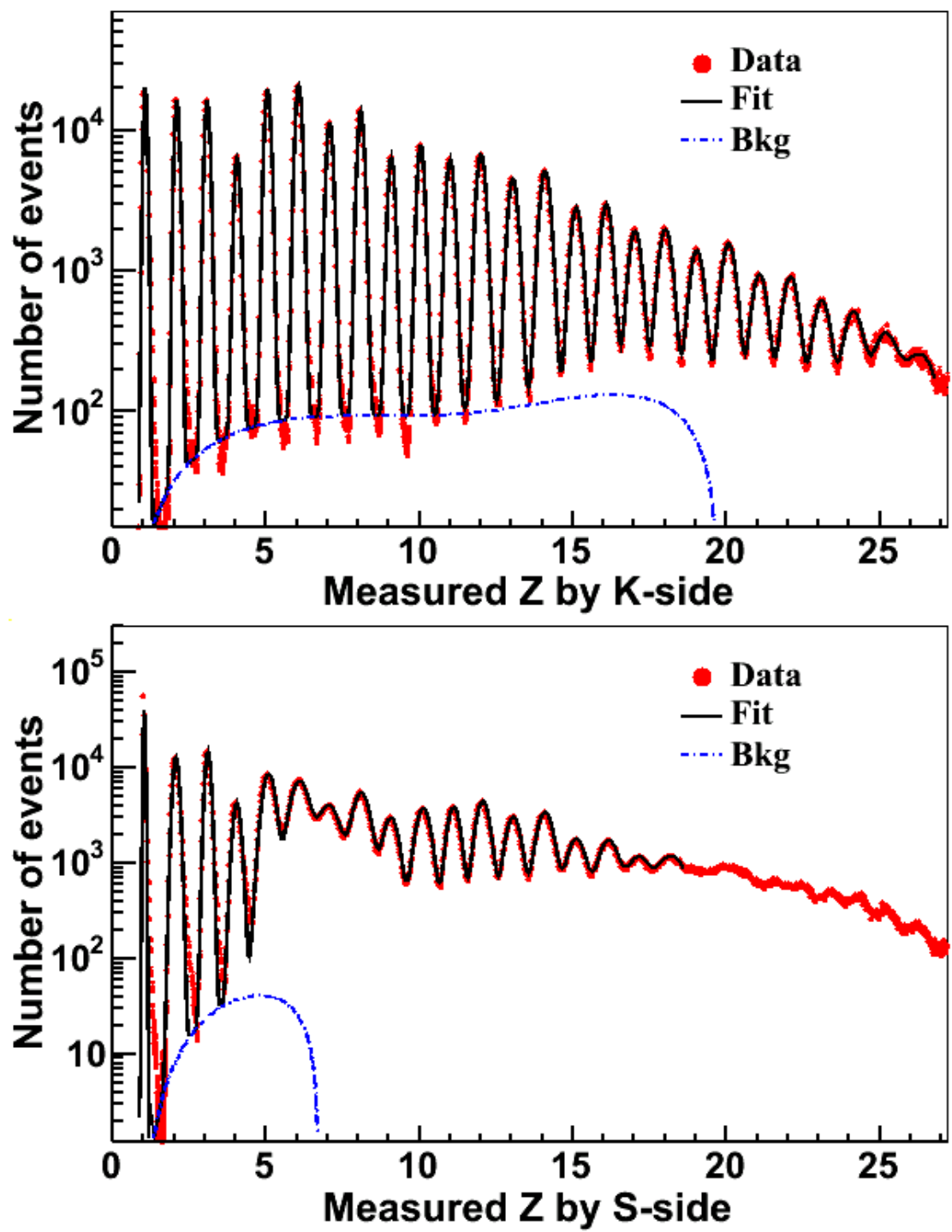


Figure 14: Combined Z measurements of six ladders at the K- and S-sides. The solid line represents a fit with the Gaussian function for each ion and the polynomial for beam fragment events and the non-Gaussian tail of each ion. The polynomial fit (bkg) is shown as a dotted-dash line.

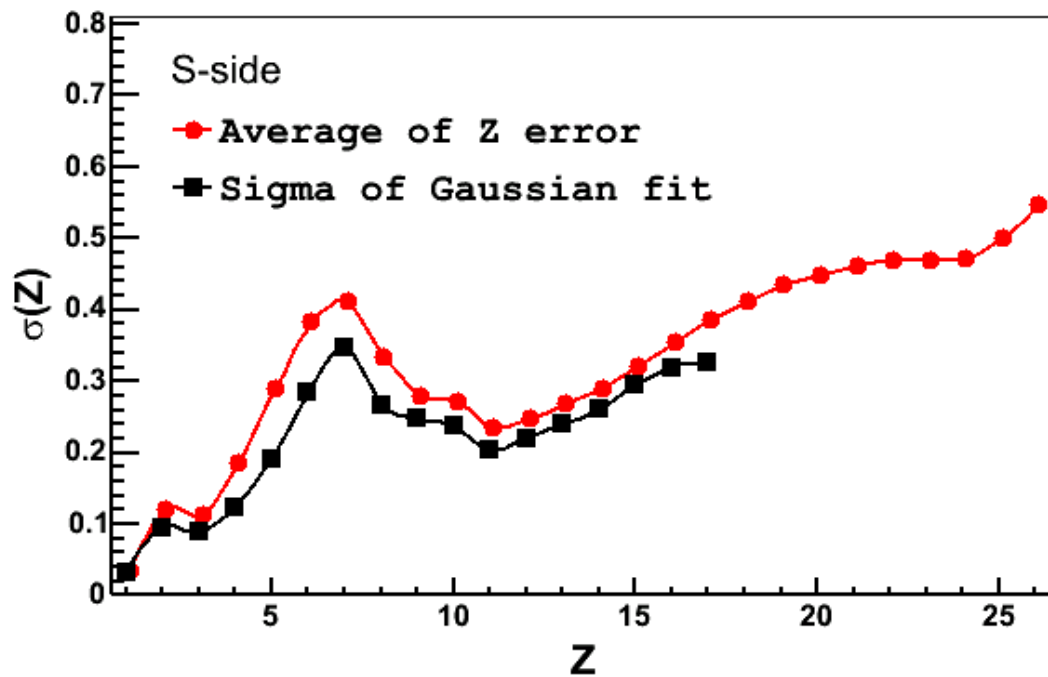
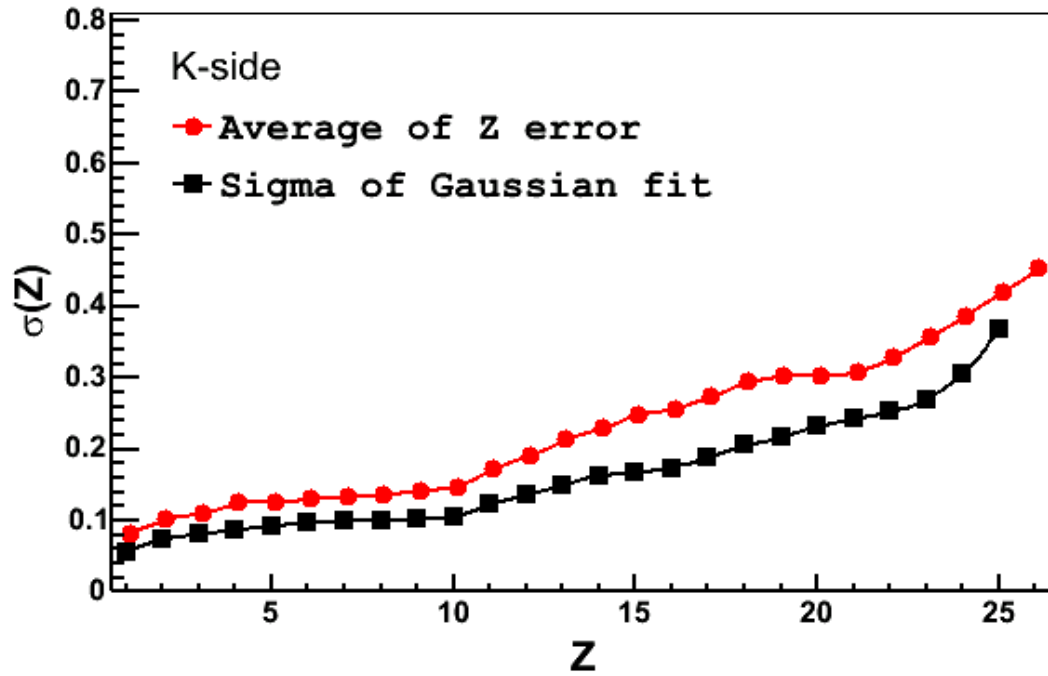


Figure 15: Comparison of the sigma of the Gaussian fit and the average error of combined Z values.

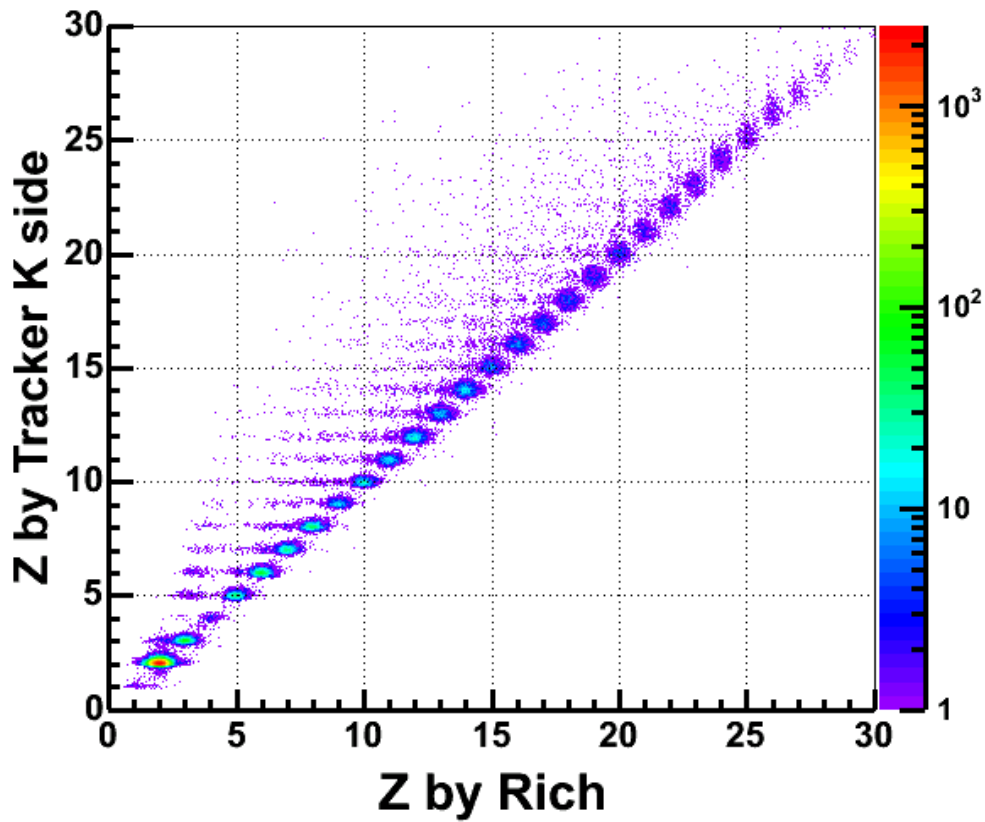
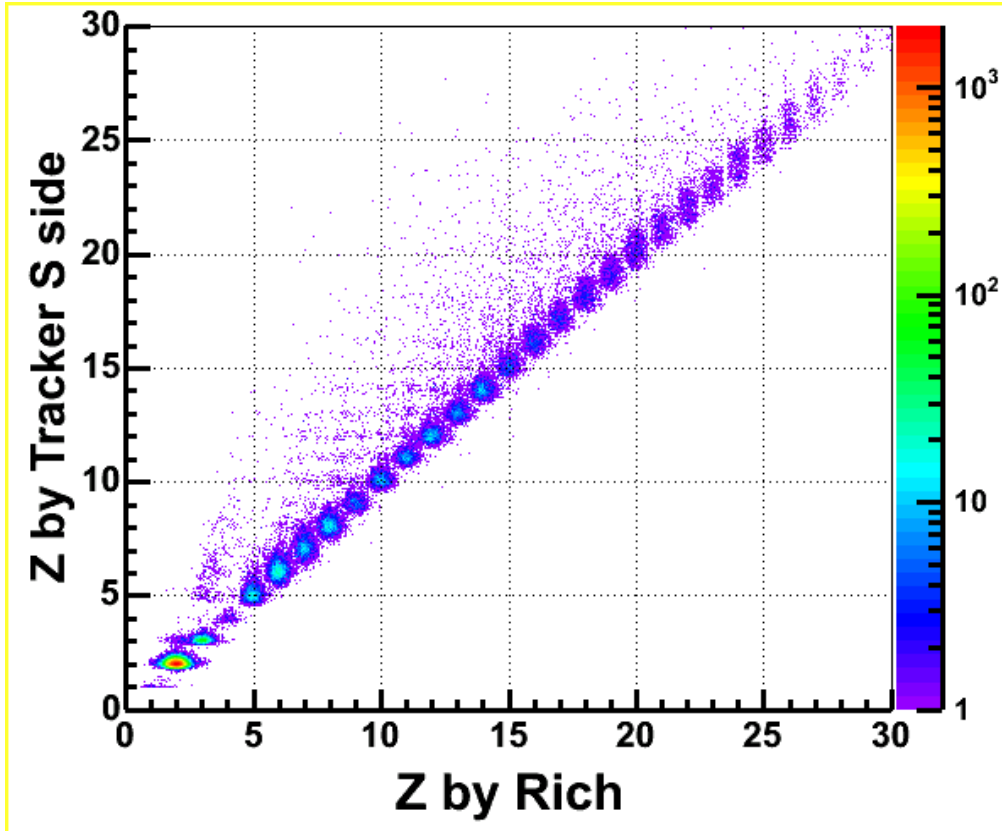


Figure 16: Correlations of measured Z values from the RICH prototype, the K- and S-sides of silicon ladders.

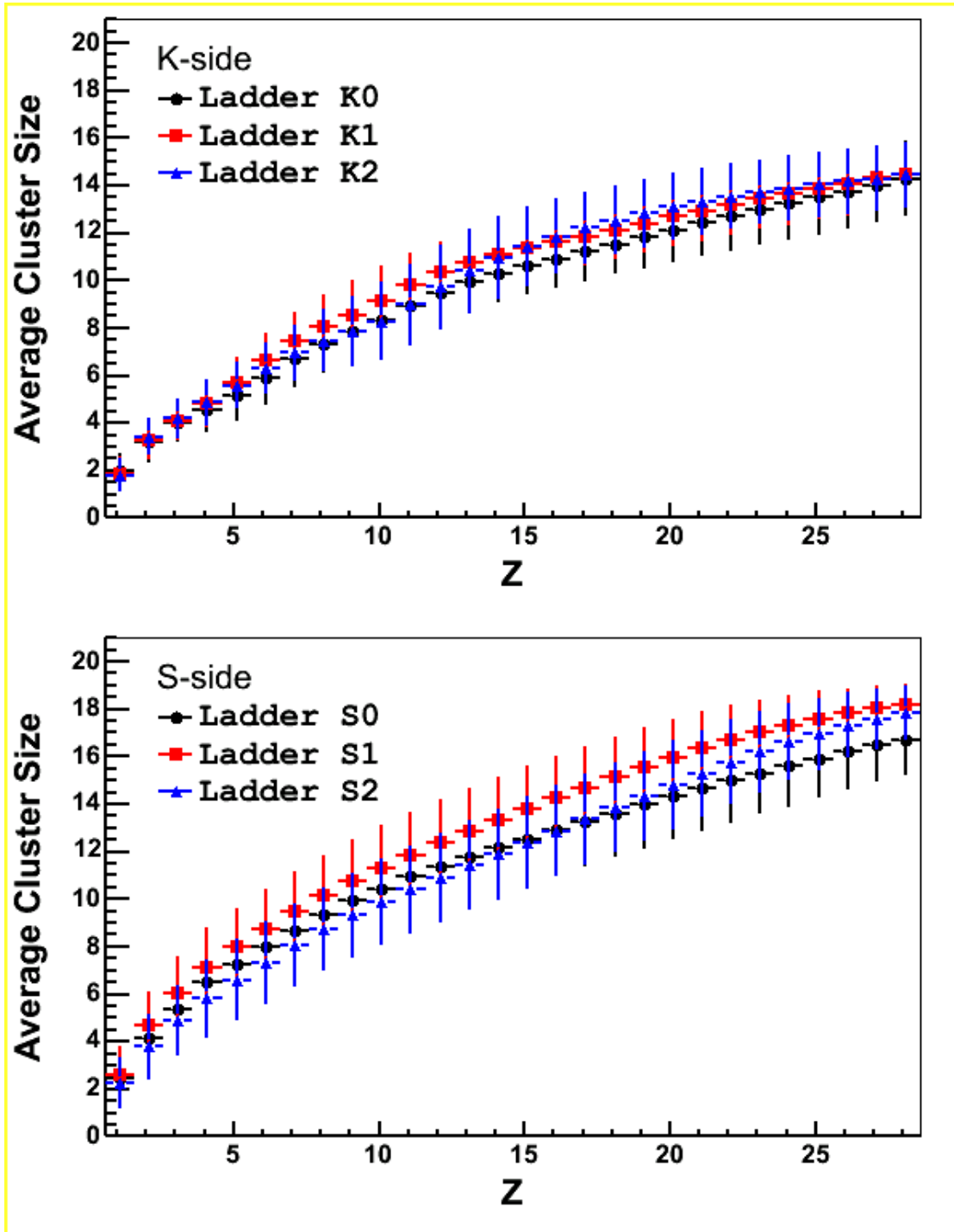


Figure 17: Average cluster size of the K- and S-sides as a function of Z. The results from three ladders are shown.